J. Water Environ. Nanotechnol., 6(3): 224-231 Summer 2021

ORIGINAL RESEARCH PAPER

Environmental-friendly synthesis of Au-Ag alloy nanoparticles using *Anethum graveolens* leaf extract and their application to Surface Enhanced Raman Scattering (SERS)

Sathyavathi Ravulapalli [1,2*] **, *Korasapati Ravichandra*** [2], ***Lankipalli Jyothi*** [1]

[1] *School of Physics, University of Hyderabad, Hyderabad-500046, India*
[2] *Department of Physics, Koneru Lakshmaiah Education Foundation, Hyderabad, Telangana-500075, India*

Received: 2021-05-28 Accepted: 2021-06-28 Published: 2021-07-01

ABSTRACT

We report an Environmental-friendly method for the synthesis of Au-Ag alloy nanoparticles (ANPs) by using Anethum graveolens fresh leaf extract as a reducing and stabilizing agent. The precursor solutions of Au ($HAuCl_4$: $3H_2O$), Ag ($AgNO_3$), and leaf extract were mixed by varying molar ratios and heated with continuous stirring at 70°C for an hour which leads to the formation of Au-Ag ANPs with different atomic compositions. The periodic observation of color changes indicated the formation of Au-Ag ANPs and got confirmed by the measurement of UV-Vis spectroscopy. The synthesized Au-Ag ANPs were characterized for morphological and elemental composition using Transmission Electron Microscopy (TEM) in conventional and scanning TEM (STEM) mode. The TEM image analysis shows that the synthesized Au-Ag ANPs were found to be spherical with a broad size distribution with a mean size of 23 ± 18 nm. The energy dispersive X-ray (EDX) spectrometry in the STEM mode confirms the formation of Au-Ag ANPs and in order to show that these biosynthesized Au-Ag ANPs could be used as SERS (Surface Enhanced Raman Scattering) substrates, we carried out SERS studies using Crystal Violet (CV) and Rhodamine 6G (R6G) as test molecules by using 514.5 nm laser excitation wavelength. The detection level achieved was 50μM of CV and R6G, which would lead to exploring biosensing applications.

Keywords: *Crystal Violet (CV), Rhodamine 6G, Scanning Transmission Electron Microscopy (STEM)*

How to cite this article
Ravulapalli S., Ravichandra K. , Jyothi L. Environmental-friendly synthesis of Au-Ag alloy nanoparticles using Anethum graveolens leaf extract and their application to Surface Enhanced Raman Scattering (SERS). J. Water Environ. Nanotechnol., 2021; 6(3): 224-231.
DOI: 10.22090/jwent.2021.03.003

INTRODUCTION

The fabrication of Bimetallic Alloy nanoparticles (ANPs) has drawn considerable attention to the field of nanotechnology. The diverse compositions and structures of bimetallic NPs can be used to integrate the functions of monometallic nanomaterials. Bimetallic Au-Ag ANPs also exhibit interesting electronic, optical, chemical, or biological properties due to the new bifunctional or synergistic effects [1–12]. Several methods [13–17] have been used in order to prepare bimetallic ANPs and most of them require reducing, capping agents, or stabilizers to control the size and composition of the ANPs. These chemical substances which are utilized in the synthesis of ANPs are toxic and a threat to the environment as well as health [18]. The development of reliable eco-friendly protocols for the synthesis of bimetallic ANPs remains a challenge. Biological systems have now emerged as a novel medium for the synthesis of various inorganic materials at a remarkably high level of complexity. Biological methods of NP synthesis using microorganisms [19–21], enzymes

* Corresponding Author Email: *sathyaravul@klh.edu.in*

[22], plants, or plant extracts [23-24] have been suggested as possible "green" alternatives to traditional chemical and physical methods due to them not requiring complex cell culture processes. In addition, methods that use plants can be suitably scaled up for large-scale NP synthesis [25]. Some reports are available on Au-Ag bimetallic nanostructures prepared using parts of the plant [26-30]. The limited number of studies is due to the more complex effects of the conditions on the rates of precursor reduction, nucleation, and growth of the alloy NPs compared with those of the conditions for monometallic NP growth. The size distribution, composition, and crystal structure of the resulting alloy NPs are difficult to control using biological methods. In this study, an environmentally benign solution method to synthesize Au-Ag ANPs using a fresh leaf extract, acting as both a reductant and a stabilizer, was developed. Various characterization techniques such as Transmission electron microscopy (TEM: using selected area diffraction and scanning TEM with energy dispersive spectroscopy and ultraviolet-visible light (UV-Vis) spectroscopy were used to confirm the nature of the ANPs. There are enormous reports available on biological applications of monometallic Au, Ag, and Bimetallic structures, Au-Ag [31-35]. The current work explores the plausibility of developing a sustainable SERS (Surface Enhanced Raman Scattering) substrate using biosynthesized Au-Ag ANPs. SERS is a prominently used technique for the detection of biomolecules due to its fingerprint-like nature [36-37]. However, the minuscule cross-sections of Raman Scattering need to be enhanced using metallic nanostructured surfaces up to a single molecule detection level [38]; hence, the SERS technique would be able to identify the extremely low concentrations of analytes in different chemical environments [39-41] and therefore, the SERS substrate plays a substantial role in the sensitivity and reproducibility of this technique. Biosynthesized metallic nanostructures for SERS applications are burgeoning areas of research; therefore, in the current study, we are preparing eco-friendly Au-Ag ANPs and exploring their application as SERS substrate that indicated promising reproducible results for their use in molecule detection at a lower concentration.

EXPERIMENTAL

(a) Materials

Silver nitrate ($AgNO_3$), and Gold (III) chloride trihydrate ($HAuCl_4.3H_2O$) were purchased from Sigma Aldrich, India.

(b) Preparation of leaf extract

The extract of *Anethum graveolens* was prepared with 10 g of fresh leaves, obtained from home premises, which were thoroughly rinsed with DDW (double distilled water) and cut into small pieces. The chopped leaves were boiled in 50 ml DDW for 15 minutes and filtered. The cooled extract was kept at 4^0 C. The filtrate is later on used as a reducing and stabilizing agent for synthesizing Au-Ag alloy NPs.

(c) Synthesis of Au- Ag alloy nanoparticles

The precursor solutions of 1mM of $AgNO_3$ and $HAuCl_4.3H_2O$ were prepared and used for the synthesis. To prepare monometallic Au and Ag nanoparticles, 2ml leaf extract is added to 20ml of each 1mM Au and Ag precursors separately at room temperature. The color change of the solution indicates the formation of Au (Pink) and Ag (yellow) NPs. These provide us to obtain monometallic Au and Ag NPs with the ratio of Au100:Ag0 and Au0:Ag100, respectively. The synthesis method [26] is modified and used in the preparation of Au-Ag ANPs. To prepare Au-Ag bimetallic alloy, nanostructures with different molar ratios typical volume of 90ml, 1mM $AgNO_3$, and $HAuCl_4$ were mixed with 10ml of leaf extract, and later on, the reaction solution was kept in a water bath at 70 degrees Centigrade with continuous stirring for 1 hour. To get the molar ratio of Au50:Ag50, 10ml of leaf extract was added to 45 ml of both Ag and Au. 60ml of Au and 30ml of Ag precursor solutions were added to 10ml leaf extract in order to obtain the ratio of Au75:Ag25 and for the ratio of Au25:Ag75, 30ml of Au precursor solution was mixed with 60ml of Ag precursor solution and 10ml leaf extract. The color change from pink to red wine color indicates the formation of the Au-Ag alloy nanoparticles. The formation of Au-Ag ANPs was monitored using Uv-visible absorption Spectroscopy.

CHARACTERIZATION

The bioreduction of pure Ag, Au, and Au-Ag ANPs of various atomic compositions was monitored by measuring the UV-Vis absorption spectra. The analysis was carried out with a JASCO UV-visible absorption spectrophotometer with a resolution of 1 nm between 300 and 900 nm

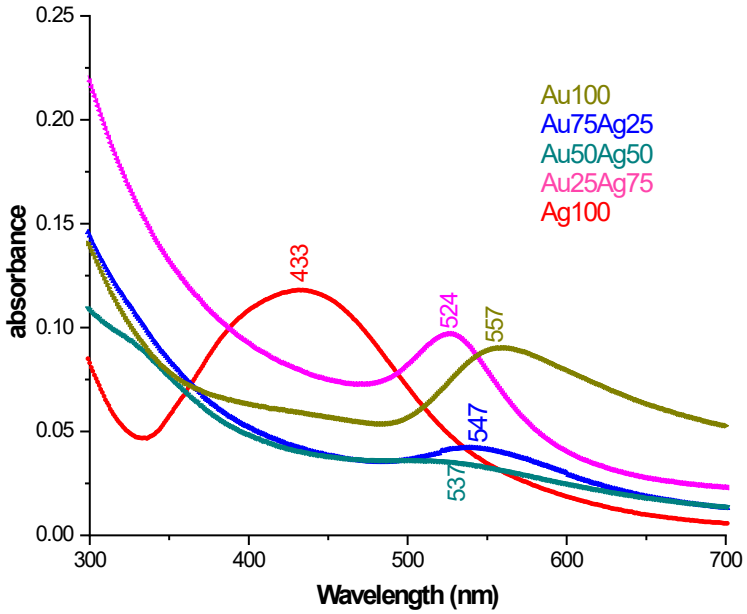

Fig. 1. UV-Vis absorption spectra of Au-Ag alloy NPs synthesized with different Au-Ag molar ratios

wavelength range. A small aliquot of 300 µL of the sample was diluted 10 times with Millipore water in order to avoid errors due to the high optical density of the solution.

The size, shape, structure, and composition of nanoparticles were carried out using a 200 keV electron beam in an Ultra High-Resolution Transmission Electron Microscope (JEOL-2010). The specimen was prepared by dispersing the nanoparticles and late on transferring them to a carbon-coated TEM grid (by drop cast method) which was subsequently dried under a 100 W lamp.

To explore the application of these eco-friendly Au-Ag, ANPs as suitable substrates for SERS. In the current study, the Au-Ag ANPs with the composition Au50:Ag50 were utilized as a substrate to detect organic dye molecules. The dye molecules such as Rhodamine 6G (R6G) and Crystal violet (CV) with high Raman scattering cross-sections have been used as probe molecules. In order to prepare the substrate, the ratio of Au-Ag nanoparticle solution to dye molecule is kept constant at 5:1. For each test, 40 µL of this solution was dropped onto the glass substrate (1X 2 cm^2) and air-dried. A fixed volume micro-pipette with disposable tips was used to prevent contamination. In our tests, the dropped solution soon spread over the whole substrate. SERS spectra were recorded using a micro-Raman spectrometer (LABRAM-HR) using laser excitation lines of 514.5. All measurements were made in backscattering geometry, using a 50 X microscope objective lens with a numerical aperture of 0.7. Typical laser power at the sample surface was 2.4 mW with a spot size of 2 µm.

RESULTS AND DISCUSSIONS

Synthesis of Au-Ag alloy NPs

Au-Ag alloy NPs were synthesized with various Au/Ag atomic ratios (100:0, 75:25, 50:50, 25:75, 0:100) by co reduction of Ag and Au precursors in the presence of Anethum graveolens fresh leaf extract at 70°C temperature for an hour. 1mM of $AgNO_3$ and $HAuCl_4$ $3H_2O$ was prepared as precursor solutions for Ag, Au, and bimetallic Au-Ag ANPs. The color formation of ANPs indicated that the leaf extract itself acted as both a reducing and a stabilizing agent. The dispersions containing pure Au nanoparticles turned from colorless to Pink while that of the solution containing pure Ag nanoparticles turned to yellow, the intermediate compositions resulted in colors varying from Pink to Violet. Temperature plays an important role in this process as it enhances the reaction rate, helps in speeding up the nuclei formation consuming metal ions, and stops the secondary reduction process of nucleation on preformed nuclei [42].

UV-Visible Spectroscopy

Figure 1 shows the UV-Vis absorption spectra

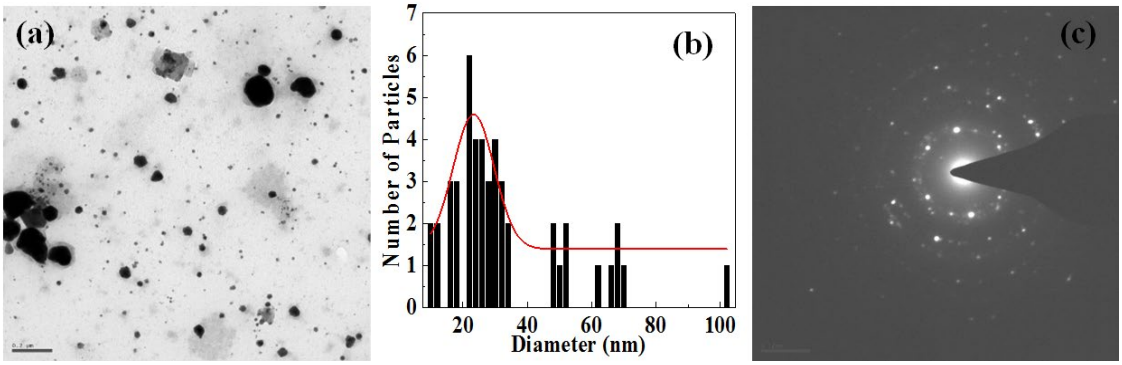

Fig. 2. (a) TEM image of Au-Ag ANPs (Au50Ag50) (b) Histogram for the Au-Ag ANPs (c) SEAD pattern of Au-Ag ANPs

of the monometallic Au, Ag, and Au-Ag ANPs with varying Au and Ag compositions. From the figure, it is observed that the Surface plasmon resonance peak for monometallic Au100 and Ag100 is centered at 557 nm and 433 nm, respectively [17]. The values of SPR peak for the Au-Ag ANps with the composition of Au75:Ag25 gives 547nm, Au50Ag50 with 537nm, and Au25Ag75 at 524nm [43]. Furthermore, it is noted that that the SPR peak of Au-Ag ANPs is decreasing with an increase in the Au composition and the values of SPR peak were obtained between that of monometallic Au and Ag. These results are in agreement with the calculated spectra of Au-Ag ANPs using Mie equations [44]. The report [45] suggests that the single monolayer of Au is sufficient to mask the plasmon resonance band of Ag completely. Due to this reason; the increased composition of Au on the particle surface resulted in diminishing the underlying Ag plasmon surface band. Furthermore, a single absorption peak for all the bimetallic nanoparticles confirms alloy formation. It cannot be obtained the either just the physical mixture of monometallic Au and Ag colloidal solution or the formation of Au-Ag Core-shell nanostructures, where there two characteristic absorption peaks are found [46-47].

Transmission Electron Microscope (TEM)

Figure 2(a) shows the typical bright-field TEM micrograph of the synthesized Au-Ag alloy NPs of Au50:Ag50 atomic ratio and from the BF images, it is clear that the shape is found to be spherical. Several such micrographs are taken at different places in the grid and through image analysis histogram, the size distribution of Au-Ag ANPs (Au50Ag50) is presented as shown in figure 2(b). (histogram). From the micrograph and the histogram shown above, the average particle size is found to be 23 ±6 nm. However, large particle sizes are also observed though their number is smaller.

Figure 2(c) depicts a selected area electron diffraction pattern from a region of interest where several Au-Ag ANPs are present. It is to be noted that Au and Ag are having FCC structures and almost very close lattice parameter. It is not possible to differentiate Au from Ag using diffraction. However, the diffraction pattern showed the reflections corresponding to (111) planes, predominantly.

STEM (TEM-EDX) elemental analysis

The scanning TEM method is powerful as the intensity is proportional to Z^2 in the annular dark field images shown in Fig 3. Fig. 3 (a-c) shows the Annulat darkfield STEM images of the Au-Ag ANPs with a variation of atomic concentrations of Au: Ag. These coloured elemental mapping images are obtained using EDS mapping in STEM mode and these images shown in Fig. 3 prove that the Au (orange), and Ag (pink) atoms were homogeneously distributed over the entire nanoparticle structure. As the signal in STEM mode mainly depends on the atomic number of elements, we observe from Figure 3 (a-c) that the strong brightness corresponds to Au (higher atomic number) and the low brightness is referred to as Ag (lower atomic number). Further, the image shows clearly the distribution of Au, Ag nanoparticles in the Au-Ag ANPs.

Figure 3a (i-iii) shows a STEM image of Au75:Ag25 composition. For elemental composition calculation, the nanoparticle highlighted in the red box from Figure 3a(i) has been considered and it is shown in figure 3a (ii). It is observed from Figure 3a(iii) that the elemental mapping of Au (87%)

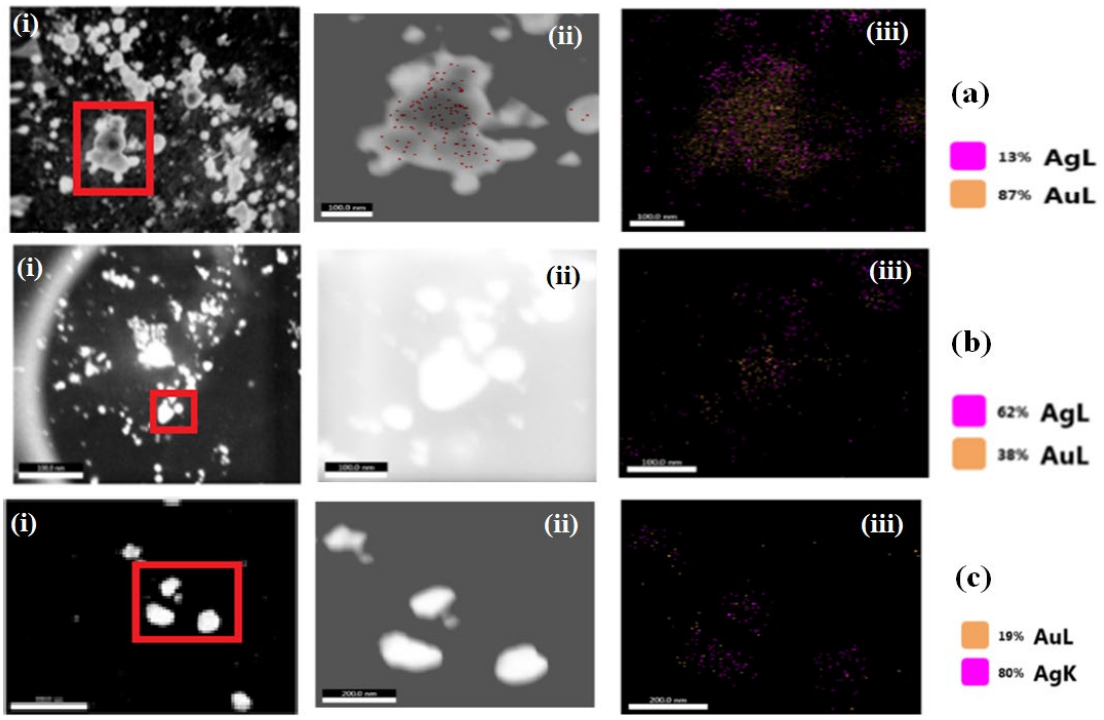

Fig. 3. Scanning TEM (STEM) image of the as-synthesized Au-Ag alloy NPs energy dispersive X-ray (EDX) elemental maps of (a) Au75: Ag25 and (b) Au50:Ag50 and (c) Au 25: Ag 75

and Ag (13%) is fairly matched with the atomic composition used in the synthesis method and was homogeneously distributed over the NP.

It is also observed from figure 3b(i-iii) that the atomic composition of Au50:Ag50 was in good agreement with the elemental mapping of Au (38%) and Ag (62%) for the highlighted nanoparticle from the figure 3 b(ii). Furthermore, from figure 3c(i-iii) the STEM image analysis shows the atomic composition of Au25:Ag75 fairly matches with Au (19%) and Ag (80%) of elemental composition from the nanoparticles of figure 3c(ii).

These results were further evidenced from Figure 4 (a-c) that EDX mapping of both the atomic percentage (%) and weight percentage (%) of Au-Ag ANPs. In the case of Au75Ag25 composition, from figure 4(a) the atomic and weight % of Au:Ag are 69:31 and 80:20 respectively which are in fair agreement with the alloyed atomic concentrations. And also, from the EDX spectra of figure 4, (b) the atomic and weight % values of Au-Ag ANPs are 45:55 and 40:60 respectively and are in good agreement with the synthesis composition of Au50Ag50. It is further observed that for the Au25Ag75 composition the EDX spectra are of the large difference in the atomic as well as weight % values 6:94 and 3:97 which could be due to the selection of Au-Ag ANP for the mapping of elemental composition.

SERS APPLICATION

Figure 5 (a) shows the SERS spectra of 50 µM concentration of CV adsorbed on Au-Ag ANPS at different locations. The sharp Raman characteristic peaks of the CV molecule have appeared at 808, 915, 1174, 1371, 1533, 1585, and 1620 cm^{-1} which are matching the reported values of one of our published reports [48]. It is well established that the size of Ag nanoclusters in the range from 50-150 nm is expected to be most efficient for signal enhancement along with the resonance effects of laser excitation wavelength and SPR peak [49]. The increased signal intensities attained for Au-Ag ANP s are attributed to the nanogaps or nano junctions which have the potential to act as hotspots for the signal enhancement. Another reason could be the resonance effect as SPR of Au-Ag ANPs at 537nm which is in resonance with the excitation of laser wavelength of 514.5nm[50-51].

From figure 5(b) it is observed that the Raman

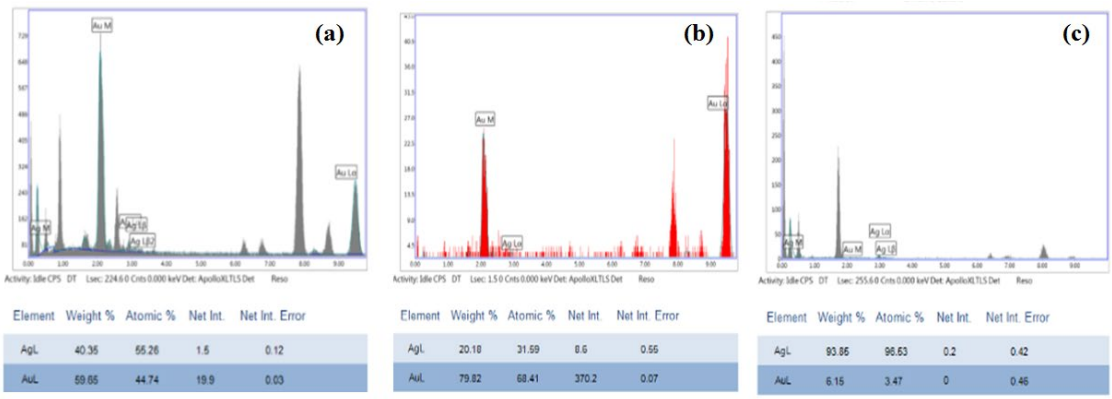

Fig. 4. EDX elemental mapping spectra of (a) Au75:Ag25 (b) Au50:Ag50 and (c) Au25:Ag 75

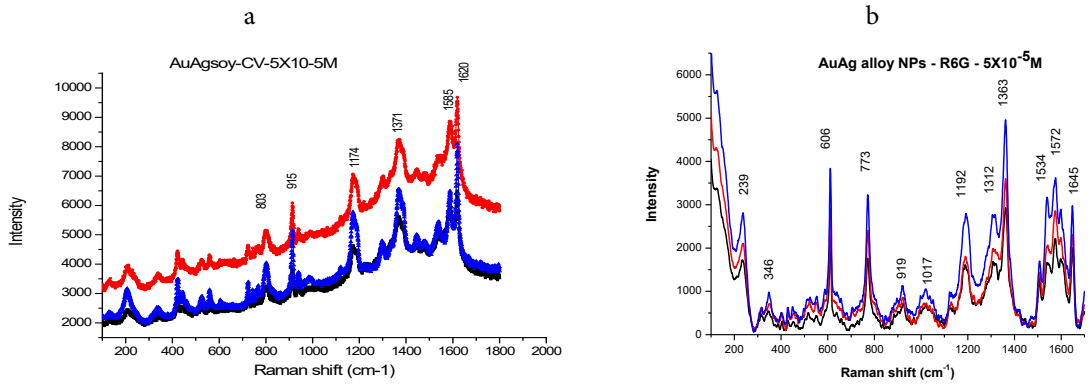

Fig. 5 (a). SERS spectra of 50 µM CV adsorbed on Au-Ag ANP s (Au50Ag50) at different locations of the sample. 5(b). The SERS spectra of 50 µM concentration R6G on eco-friendly Au- Ag alloy nanoparticles (Au50:Ag 50) on glass substrate.

signals at about 606, 768, 1194, 1363, 1534, 1572, and 1645 cm^{-1} which are the characteristic Raman peaks of R6G [47-48]. It is reported that the Raman peaks at 606, 768, and 1194 cm^{-1} are associated with the vibration modes of analyte molecular R6G as C–C–C ring in-plane, C–H out of plane bend mode and C–C stretching vibrations, respectively. The peaks at 1361, 1503, 1534, and 1646 cm^{-1} are arising from symmetric modes of in-plane C–C stretching vibrations of R6G because of the resonance enhancement effect at 514.5 nm excitation [49]. The marked peak positions in Figure 5(b) are consistent with the previous reports on R6G [48].

In the field of SERS, one of the major problems is the reproducibility of the SERS spectra, as the spectra depend on the shape, size of the metal nanoparticles, and the orientation of adsorbed molecule on the metal nanoparticle. We have recorded the SERS spectra several times and at several positions of the same substrate, the observed spectra were almost identical. We could reproducibly obtain all the Raman peaks except for certain broad structures appearing which might be due to some impurity molecules adhering to the substrate while recording the spectra. From these observations, we can conclude that reproducibility is better with these substrates. Moreover, in the present study, we have obtained the concentration detection limit as 50 µM, which would allow us to explore biosensing applications in future experiments.

CONCLUSIONS

An alternative solution for the synthesis of Au-Ag alloy NPs with controlled compositions was developed using an Anethum graveolens leaf extract as both reductant and stabilizer. The mixture of preformed Au and Ag NPs with

optimized molar ratios at 70^{0}C temperature is suitable for the one-pot synthesis of the Au-Ag alloy nanoparticles. TEM, STEM, and EDX spectra results confirm the alloy formation. The proposed method is simple eco-friendly and cost-effective as it does not require an extra surfactant or reductant. This reported synthetic method represents a new approach to the synthesis of alloy-structured NPs for the potential application in SERS (Surface Enhanced Raman Scattering). The minimum possible concentration of detectable CV and R6G was down to 50µM would lead to exploring further biosensing applications.

ACKNOWLEDGMENTS

R. Sathyavathi greatly acknowledges financial support from the **DST-PURSE fellowship from the University of Hyderabad** provided for this work. K. Ravichandra acknowledges financial support from the DBT-JRF fellowship. The authors greatly acknowledge the STEM facilities provided by the Center for Nanotechnology, University of Hyderabad, Hyderabad, India.

CONFLICTS OF INTEREST

The authors declare there are no conflicts of interest.

REFERENCES

1. Daniel M-C, Astruc D. Gold Nanoparticles: Assembly, Supramolecular Chemistry, Quantum-Size-Related Properties, and Applications toward Biology, Catalysis, and Nanotechnology. Chemical Reviews. 2004;104(1):293-346.
2. Hostetler MJ, Zhong C-J, Yen BKH, Anderegg J, Gross SM, Evans ND, et al. Stable, Monolayer-Protected Metal Alloy Clusters. Journal of the American Chemical Society. 1998;120(36):9396-7.
3. Mallin MP, Murphy CJ. Solution-Phase Synthesis of Sub-10 nm Au–Ag Alloy Nanoparticles. Nano Letters. 2002;2(11):1235-7.
4. Treguer M, de Cointet C, Remita H, Khatouri J, Mostafavi M, Amblard J, et al. Dose Rate Effects on Radiolytic Synthesis of Gold–Silver Bimetallic Clusters in Solution. The Journal of Physical Chemistry B. 1998;102(22):4310-21.
5. Kelly KL, Coronado E, Zhao LL, Schatz GC. The Optical Properties of Metal Nanoparticles: The Influence of Size, Shape, and Dielectric Environment. The Journal of Physical Chemistry B. 2002;107(3):668-77.
6. Schmid G, West H, Mehles H, Lehnert A. Hydrosilation Reactions Catalyzed by Supported Bimetallic Colloids. Inorganic Chemistry. 1997;36(5):891-5.
7. Shi H, Zhang L, Cai W. Composition modulation of optical absorption in AgxAu1−x alloy nanocrystals in situ formed within pores of mesoporous silica. Journal of Applied Physics. 2000;87(3):1572-4.
8. Shibata T, Bunker BA, Zhang Z, Meisel D, Vardeman CF, Gezelter JD. Size-Dependent Spontaneous Alloying of Au–Ag Nanoparticles. Journal of the American Chemical Society. 2002;124(40):11989-96.
9. Moskovits M, Srnová-Šloufová I, Vlčková B. Bimetallic Ag–Au nanoparticles: Extracting meaningful optical constants from the surface-plasmon extinction spectrum. The Journal of Chemical Physics. 2002;116(23):10435-46.
10. Zhong CJ, Maye MM. Core-Shell Assembled Nanoparticles as Catalysts. Advanced Materials. 2001;13(19):1507-11.
11. Habas SE, Lee H, Radmilovic V, Somorjai GA, Yang P. Shaping binary metal nanocrystals through epitaxial seeded growth. Nature Materials. 2007;6(9):692-7.
12. Davis RJ, Boudart M. Structure of Supported PdAu Clusters Determined by X-ray Absorption Spectroscopy. The Journal of Physical Chemistry. 1994;98(21):5471-7.
13. Raveendran P, Fu J, Wallen SL. A simple and "green" method for the synthesis of Au, Ag, and Au–Ag alloy nanoparticles. Green Chem. 2006;8(1):34-8.
14. Liu X, Wang A, Yang X, Zhang T, Mou C-Y, Su D-S, et al. Synthesis of Thermally Stable and Highly Active Bimetallic Au–Ag Nanoparticles on Inert Supports. Chemistry of Materials. 2008;21(2):410-8.
15. Liu J-H, Wang A-Q, Chi Y-S, Lin H-P, Mou C-Y. Synergistic Effect in an Au–Ag Alloy Nanocatalyst: CO Oxidation. The Journal of Physical Chemistry B. 2005;109(1):40-3.
16. Wang D, Li Y. Bimetallic Nanocrystals: Liquid-Phase Synthesis and Catalytic Applications. Advanced Materials. 2011;23(9):1044-60.
17. Senapati S, Ahmad A, Khan MI, Sastry M, Kumar R. Extracellular Biosynthesis of Bimetallic Au-Ag Alloy Nanoparticles. Small. 2005;1(5):517-20.
18. Gan PP, Ng SH, Huang Y, Li SFY. Green synthesis of gold nanoparticles using palm oil mill effluent (POME): A low-cost and eco-friendly viable approach. Bioresource Technology. 2012;113:132-5.
19. Klaus T, Joerger R, Olsson E, Granqvist CG. Silver-based crystalline nanoparticles, microbially fabricated. Proceedings of the National Academy of Sciences. 1999;96(24):13611-4.
20. Konishi Y, Ohno K, Saitoh N, Nomura T, Nagamine S, Hishida H, et al. Bioreductive deposition of platinum nanoparticles on the bacterium Shewanella algae. Journal of Biotechnology. 2007;128(3):648-53.
21. Nair B, Pradeep T. Coalescence of Nanoclusters and Formation of Submicron Crystallites Assisted by Lactobacillus Strains. Crystal Growth & Design. 2002;2(4):293-8.
22. Willner I, Baron R, Willner B. Growing Metal Nanoparticles by Enzymes. Advanced Materials. 2006;18(9):1109-20.
23. Nagababu U, Boddeti G, Diwakar B.S, Chatterjee A. International Journal of Scientific & Technology Research.2019; 8(11): 1411-1414.
24. Kandula V, Balakrishna C, Behera M, Nagababu U, Kumar GK, Chatterjee A. Catalytic Efficiency of Biosynthesized Silver Nanoparticles in Synthesis of Chromones and Reduction of Nitro Aromatics. ChemistrySelect. 2019;4(48):14043-9.
25. Mondal B, Saha SK. Fabrication of SERS substrate using nanoporous anodic alumina template decorated by silver nanoparticles. Chemical Physics Letters. 2010;497(1-3):89-93.
26. AbdelHamid AA, Al-Ghobashy MA, Fawzy M, Mohamed MB, Abdel-Mottaleb MMSA. Phytosynthesis of Au, Ag, and Au–Ag Bimetallic Nanoparticles Using Aqueous Extract of Sago Pondweed (Potamogeton pectinatus L.). ACS Sustainable Chemistry & Engineering. 2013;1(12):1520-9.
27. Song JY, Kim BS. Biological synthesis of bimetallic Au/

Ag nanoparticles using Persimmon (Diopyros kaki) leaf extract. Korean Journal of Chemical Engineering. 2008;25(4):808-11.
28. Shore MS, Wang J, Johnston-Peck AC, Oldenburg AL, Tracy JB. Synthesis of Au(Core)/Ag(Shell) Nanoparticles and their Conversion to AuAg Alloy Nanoparticles. Small. 2010;7(2):230-4.
29. Mondal S, Roy N, Laskar RA, Sk I, Basu S, Mandal D, et al. Biogenic synthesis of Ag, Au and bimetallic Au/Ag alloy nanoparticles using aqueous extract of mahogany (Swietenia mahogani JACQ.) leaves. Colloids and Surfaces B: Biointerfaces. 2011;82(2):497-504.
30. Garcia AG, Lopes PP, Gomes JF, Pires C, Ferreira EB, Lucena RGM, et al. Eco-friendly synthesis of bimetallic AuAg nanoparticles. New J Chem. 2014;38(7):2865-73.
31. Hu X, Xu X, Fu F, Yang B, Zhang J, Zhang Y, et al. Synthesis of bimetallic silver-gold nanoparticle composites using a cellulose dope: Tunable nanostructure and its biological activity. Carbohydrate Polymers. 2020;248:116777.
32. Liu L, Koushki E, Tayebee R. Surface modification of gold nanoparticles by cetirizine through surface plasmon resonance and preliminary study of the in vitro cellular cytotoxicity. Journal of Molecular Liquids. 2021;330:115542.
33. Hoseininasr AS, Tayebee R. Synthesis and characterization of superparamagnetic nanohybrid Fe3 O4 /NH2 -Ag as an effective carrier for the delivery of acyclovir. Applied Organometallic Chemistry. 2018;32(12):e4565.
34. Gao H, Tayebee R, Abdizadeh MF, Mansouri E, Latifnia M, Pourmojahed Z. The efficient biogeneration of Ag and NiO nanoparticles from VPLE and a study of the anti-diabetic properties of the extract. RSC Advances. 2020;10(5):3005-12.
35. Mohammadzadeh Kakhki R, Tayebee R, Ahsani F. New and highly efficient Ag doped ZnO visible nano photocatalyst for removing of methylene blue. Journal of Materials Science: Materials in Electronics. 2017;28(8):5941-52.
36. Shmarakov I, Mukha I, Vityuk N, Borschovetska V, Zhyshchynska N, Grodzyuk G, et al. Antitumor Activity of Alloy and Core-Shell-Type Bimetallic AgAu Nanoparticles. Nanoscale Research Letters. 2017;12(1).
37. Petry R, Schmitt M, Popp J. Raman Spectroscopy-A Prospective Tool in the Life Sciences. ChemPhysChem. 2002;4(1):14-30.
38. Jonáš A, De Luca AC, Pesce G, Rusciano G, Sasso A, Caserta S, et al. Diffusive Mixing of Polymers Investigated by Raman Microspectroscopy and Microrheology. Langmuir. 2010;26(17):14223-30.
39. De Luca AC, Reader-Harris P, Mazilu M, Mariggiò S, Corda D, Di Falco A. Reproducible Surface-Enhanced Raman Quantification of Biomarkers in Multicomponent Mixtures. ACS Nano. 2014;8(3):2575-83.
40. Auchinvole CAR, Richardson P, McGuinnes C, Mallikarjun V, Donaldson K, McNab H, et al. Monitoring Intracellular Redox Potential Changes Using SERS Nanosensors. ACS Nano. 2011;6(1):888-96.
41. Yang Y, Shi J, Kawamura G, Nogami M. Preparation of Au–Ag, Ag–Au core–shell bimetallic nanoparticles for surface-enhanced Raman scattering. Scripta Materialia. 2008;58(10):862-5.
42. Song JY, Kim BS. Rapid biological synthesis of silver nanoparticles using plant leaf extracts. Bioprocess and Biosystems Engineering. 2008;32(1):79-84.
43. Link S, Wang ZL, El-Sayed MA. Alloy Formation of Gold–Silver Nanoparticles and the Dependence of the Plasmon Absorption on Their Composition. The Journal of Physical Chemistry B. 1999;103(18):3529-33.
44. Mulvaney P. Surface Plasmon Spectroscopy of Nanosized Metal Particles. Langmuir. 1996;12(3):788-800.
45. Mulvaney P, Giersig M, Henglein A. Electrochemistry of multilayer colloids: preparation and absorption spectrum of gold-coated silver particles. The Journal of Physical Chemistry. 1993;97(27):7061-4.
46. Mallik K, Mandal M, Pradhan N, Pal T. Seed Mediated Formation of Bimetallic Nanoparticles by UV Irradiation: A Photochemical Approach for the Preparation of "Core–Shell" Type Structures. Nano Letters. 2001;1(6):319-22.
47. Liu, Guyot-Sionnest P. Synthesis and Optical Characterization of Au/Ag Core/Shell Nanorods. The Journal of Physical Chemistry B. 2004;108(19):5882-8.
48. Botta R, Upender G, Sathyavathi R, Narayana Rao D, Bansal C. Silver nanoclusters films for single molecule detection using Surface Enhanced Raman Scattering (SERS). Materials Chemistry and Physics. 2013;137(3):699-703.
49. Upender G, Satyavathi R, Raju B, Shadak Alee K, Narayana Rao D, Bansal C. Silver nanocluster films as novel SERS substrates for ultrasensitive detection of molecules. Chemical Physics Letters. 2011;511(4-6):309-14.
50. Michaels AM, Jiang, Brus L. Ag Nanocrystal Junctions as the Site for Surface-Enhanced Raman Scattering of Single Rhodamine 6G Molecules. The Journal of Physical Chemistry B. 2000;104(50):11965-71.
51. Tiwari VS, Oleg T, Darbha GK, Hardy W, Singh JP, Ray PC. Non-resonance SERS effects of silver colloids with different shapes. Chemical Physics Letters. 2007;446(1-3):77-82.